Theory of water and charged liquid bridges

K. Morawetz[1,2,3]
[1] *Münster University of Applied Science, Stegerwaldstrasse 39, 48565 Steinfurt, Germany*
[2] *International Institute of Physics (IIP), Universidade Federal do Rio grande do Norte - UFRN, Brazil and*
[3] *Max-Planck-Institute for the Physics of Complex Systems, 01187 Dresden, Germany*

The phenomena of liquid bridge formation due to an applied electric field is investigated. A new solution for the charged catenary is presented which allows to determine the static and dynamical stability conditions where charged liquid bridges are possible. The creeping height, the bridge radius and length as well as the shape of the bridge is calculated showing an asymmetric profile in agreement with observations. The flow profile is calculated from the Navier Stokes equation leading to a mean velocity which combines charge transport with neutral mass flow and which describes recent experiments on water bridges.

PACS numbers: 05.60.Cd, 47.57.jd,47.65.-d, 83.80.Gv,

I. INTRODUCTION

The formation of a water bridge between two beakers when high electric fields are applied is a phenomenon known since over 100 years [1]. It has remained attractive to current experimental activities [2, 3]. On one side the properties of water are such complex that the complete microscopic theory of this effect is still lacking. On the other side the formation of water bridges on nanoscales are of current interest both from fundamental understanding of electrohydrodynamics and from applications ranging from atomic force microscopy [4] to electrowetting problems [5]. Microscopically the nanoscale wetting is of importance to confine chemical reactions [6] which reveals an interesting interplay between field-induced polarization, the surface tension, and condensation [7, 8].

Molecular dynamical simulations have been performed in order to explore the mechanism of water bridges at the molecular level leading to the formation of aligned dipolar filaments that bridges boundaries of nanoscale confinements [9]. A competition was found of orientation of molecular dipoles and the electric field leading to a threshold where the rise of a pillar overcomes the surface tension [8]. In this respect the understanding of the microscopic structure is essential for such phenomena in micro-fluidics [10]. The problem is connected with the dynamics of charged liquids which is important for capillary jets [11], current applications in ink printers and electrosprays [12, 13]. Consequently the nonlinear dynamics of breakup of free surfaces and flows has been studied intensively [14, 15].

Much physical insight can be gained already on the macroscopic scale, where the phenomena of liquid bridging is not restricted to water but can be observed in other liquids too [16] which shows that it has its origin in electrohydrodynamics [17] rather then in molecular-specific structures. The traditional treatment is based on the Maxwell pressure tensor where the electric field effects comes from the ponderomotoric forces and due to boundary conditions of electrodynamics [18]. This is based exclusively on the fact that bulk-charge states decay on a time scale of the dielectric constant divided by the conductivity, $\epsilon\epsilon_0/\sigma$ which takes for pure water 0.14ms. This decay-time of bulk charges follows from the continuity of charge density $\dot\rho_c = -\nabla\cdot\mathbf{j}$ combined with Ohm's law $\mathbf{j}=\sigma\mathbf{E}=-\sigma\nabla\phi$ where the source of the electric field is given by the potential $\nabla^2\phi=-\rho_c/\epsilon\epsilon_0$. An overview about the different forces occurring in microelectrode structures are discussed in [19].

However this simple Ohm picture leads to problems in charged liquids. It suggests a constant velocity or current of charged particles caused by the external field. On the other hand the total current of the mass motion cannot be constant but is dependent on the area where it is forced to flow through for incompressible fluids. Here in this paper we will present a discussion of this seemingly contradiction in pictures leading to a dynamical stability criterion for the water bridge and a combined flow expression. This is in line with the idea of [17] where the bulk charges have been assumed to be realized in a surface sheet.

In the absence of bulk charges the forces on the water stream are caused by the pressure due to the polarizability of the water described by the high dielectric susceptibility ϵ. This pressure leads to the catenary form of water bridge like a hanging robe [20]. While already the simplified model of [16] employing a capacitor picture leads to a critical field strength for the formation of the water bridge, the catenary model [20] has not been reported to yield such a critical field. In this paper we will show that the uncharged catenary provides indeed a minimal critical field strength for the water bridge formation in dependence on the length of the bridge. This critical field strength is modified if charges are present in the bridge which we will present here with the help of a new charged catenary solution. This allows also to explain the asymmetry found in the bridge profile [3].

density	ρ	=	10^3kg/m^3
dielectric susceptibility	ϵ	=	81
surface tension	σ_s	=	7.27×10^{-2}N/m
viscosity	η	=	1.5×10^{-3}Ns/m^2
conductivity of clean water	σ_0	=	5×10^{-6}A/Vm
molecular conductivity of NaCl	λ	=	12.6×10^{-3}Am^2/Vmol
heat capacity	c_p	=	4.187 J/gK

TABLE I: Variables and parameters used within this paper for water.

II. OVERVIEW ABOUT THE PAPER

In addition to the approaches discussed so far we want to advocate the following picture. Imaging to make a snapshot of the charges flowing through the bridge we could not decide whether the charge is due to bulk charges or due to the floating motion of charges. This flow of charges within the liquid bridge we can associate with a dynamical bulk charge of mass motion which is not covered by the decay of bulk charges discussed above. This picture is supported by the experimental observation of possible copper ion motion [21] and by the observation that the water bridge is highly sensitive to additional external electric fields [22] and strong fields even create small cone jets [2]. This dynamical bulk charge will lead to the problem of a charged catenary. Though charged membranes have been discussed in the literature [23], the analytical solutions of the charged catenary presented in this paper is unknown to the authors knowledge.

That the simple model of Ohmic resistors and capacitor as described above is not sufficient one can see from the observation that adding a small amount of electrolytes to the clean water destroys the water bridge almost immediately. In other words well conducting liquids should not perform a water bridge. In the presented model here we will derive an upper bound for the charges possibly carried in the water in order to remain in stable liquid bridges. Though we present all calculations for water parameters summarized in table I, the theory applies as well to any dielectric liquid in electric fields.

The scenario of water or other dielectric bridges happens as follows. Applying an electric field the water creeps up the beaker and form a bridge as it is nicely pictured in [2]. This bridge can be elongated up to a critical field strength and it forms a catenary which becomes asymmetric for higher gravitation to electric field ratios [3]. The critical value for stability is sensitively dependent on ion concentrations breaking off at very low concentrations. The amount of mass flow through the bridge does not follow simple Ohmic transport as we will see in this paper.

Therefore, four theoretical questions have to be answered: (i) How is the electric field influencing the height water can creep up? (ii) What radius has the bridge? (iii) What form has the water bridge? What are the static constraints on the bridge. (iv) What dynamical constraints can be found for possible bridge formation.

We will address all four questions with the help of four parameters composed of the properties summarized in table I of water. The first one is the capillary height

$$a = \sqrt{\frac{2\sigma_s}{\rho g}} = 3.8\,\mathrm{mm} \tag{1}$$

the second parameter is the water column height balancing the dielectric pressure calling creeping height in the following

$$b(E) = \frac{\epsilon_0(\epsilon-1)E^2}{\rho g} = 7.22\bar{E}^2\,\mathrm{cm} \tag{2}$$

where the electric field is in units of $[\bar{E}] = 10^4$V/cm. The third one is the dimensionless ratio of the force density on the charges by the field to the gravitational force density

$$c(\rho_c, E) = \frac{\rho_c E}{\rho g} = 15.97\bar{E}\bar{\rho}_c \tag{3}$$

where the charge density is in units of $[\bar{\rho}_c] = ng/l$. For dynamical consideration the characteristic velocity

$$u_0 = \frac{\rho g a^2}{32\eta} \approx 3.02\mathrm{m/s} \tag{4}$$

will be useful to introduce.

The outline of the paper is as follows. In the next chapter we repeat shortly the standard treatment of creeping height and bubble radius calculation of a liquid but add the pressure by the external electric field on the dielectric liquid. Then we present the form of the bridge in terms of a new solution of the catenary equation due to bulk charges in chapter IV. In chapter V we present the flow calculation proposing the picture of moving charged particles due to the field which drag the neutral particles. This will lead to a dynamical stability criterion. Summary and conclusion ends up the discussion in chapter VI.

III. FORMATION OF BRIDGE: CREEPING HEIGHT, RADIUS

We start to calculate the possible creeping height. Therefore we use the pressure tensor for dielectric media [18]

$$\sigma^{ik} = -p\delta_{ik} - \sigma_s\left(\frac{1}{R_1}+\frac{1}{R_2}\right) + \epsilon\epsilon_0 E_i E_k - \frac{1}{2}\tilde{\epsilon}\epsilon_0 E^2\delta_{ik} \tag{5}$$

where p is the pressure in the system, R_1, R_2 the principal radii of curvature such that the second term on the right hand side describe the contribution due to surface tension and the last terms are the parts due to forces in the dielectric medium. We assume a density-homogeneous

liquid such that $\tilde{\epsilon} = \epsilon - n(d\epsilon/dn)_T \approx \epsilon$. Denoting the normal vectors by e_i, the stability condition between water (W) and air (L) is given by

$$\sigma^{ik}_{(L)} e^k_{(L)} = -\sigma^{ik}_{(W)} e^k_{(W)} = -\sigma^{ik}_{(L)} e^k_{(W)}. \tag{6}$$

Since the principal curvature is much larger radially to the tube than parallel, we have $R_2 \sim \infty$ and denoting the coordinate in the direction of the height with z, the pressure difference between water and air is $p_W - p_L = \rho g z$. The balance (6) with (5) reads then

$$\rho g z + \frac{\sigma_s}{R_1} = \frac{1}{2}\epsilon_0(\epsilon - 1)(\epsilon E_n^2 + E_t^2). \tag{7}$$

Here we have employed the boundary conditions for the normal and tangential components of the electric field

$$E^n_{(L)} = \epsilon E^n_{(W)} = \epsilon E_n, \qquad E^t_{(L)} = E^t_{(W)} = E_t. \tag{8}$$

We assume the electric field in x-direction such that $E_t = -E\cos\alpha$, $E_n = E\sin\alpha$ where $z'(x) = \tan\alpha$ is the increase of the surface line of the water. Using the parameters (1) and (2) we obtain from the stability condition (7) the differential equation

$$2z - a^2 \frac{z''}{(1+z'^2)^{3/2}} = \epsilon_0(\epsilon - 1)(\epsilon E_n^2 + E_t^2) \approx b \tag{9}$$

where we used the approximation of small normal electric fields justified if there are no surface charges. This shows the modification of the standard treatment of capillary height by the applied field condensed on the right hand side. The first integral of (9) is

$$\frac{z^2}{a^2} + \frac{1}{\sqrt{1+z'^2}} - \frac{bz}{a^2} = 1 \tag{10}$$

where we used the condition that for $x \to \infty$ $z = z' = 0$. The explicit solution of the surface curve $z(x)$ is quite lengthy and not necessary here. Instead we can give directly the maximally reachable height in dependence on the electric field. Therefore we use the angle $\theta = 90 - \alpha$ of the liquid surface with the wall such that $z'(x) = -\cot\theta$ and from (10) we obtain

$$z = \frac{b}{2} + \sqrt{\frac{b^2}{4} + a^2(1-\sin\theta)} \le \frac{b}{2} + \sqrt{\frac{b^2}{4} + a^2} = z_{\max} \tag{11}$$

which shows that without electric field the maximal creeping height is just the capillary length (1) as it is well known. The other extreme of very high fields leads to the field-dependent length (2) which justifies the name creeping height. This answers the first question concerning creep heights.

The second question concerning the radius of the bridge one finds by equating the pressure of surface tension with the gravitational force density

$$\frac{\sigma_s}{R} = \rho g z \approx \rho g 2R \tag{12}$$

such that the radius of the water bridge is at the beaker

$$R \approx a/2. \tag{13}$$

Without using the approximation we could express the curvature again by differential expressions in $z(x)$ defining a radial profile, as it can be found in text books [18].

IV. LIQUID BRIDGE: BRIDGE SHAPE

A. Charged catenary

Now we turn to the question which form the water bridge will take. Therefore we consider the center of mass line of the bridge being described by $z = f(x)$ with the ends at $f(0) = f(L) = 0$. The force densities are multiplied with the area and the length element $ds = \sqrt{1+f'^2}dx$ to form the free energy. We have the gravitational force density$\rho g f$ and the volume tension $\rho g b$ as well as the force density by dynamical charges $\rho_c E x$ which contributes. The surface tension is negligible here. The form of the bridge will be then determined by the extreme value of the free energy

$$\int_0^L \mathcal{F}(x)dx = \rho g \int_0^L (f(x) + b - cx)\sqrt{1+f'^2}dx \to extr. \tag{14}$$

where c is given by (3) and b defined in (2). Introducing $t(x) = f(x) + b - cx$, the corresponding Lagrange equation possesses a first integral

$$t'(x)\frac{\partial \mathcal{F}}{\partial t'(x)} - \mathcal{F} = -\xi\sqrt{1+c^2}. \tag{15}$$

The resulting differential equation is solved in an implicit way

$$t(x) = \xi\cosh\frac{1}{\xi}(x(1+c^2) + ct(x) - c_1) \tag{16}$$

with the integration constants ξ, c_1 to be determined by the boundary conditions $f(0) = f(L) = 0$. Renaming variables the solution can be represented parametrically as

$$\begin{aligned} f(t) &= \frac{1}{1+c^2}\left\{ct + \xi\left[\cosh\left(\frac{t}{\xi} - \frac{Ld}{2\xi}\right) - \cosh\left(\frac{Ld}{2\xi}\right)\right]\right\} \\ x(t) &= t - cf(t), \qquad t \in (0, L). \end{aligned} \tag{17}$$

The boundary conditions lead to

$$d = 2\frac{\xi}{L}\mathrm{arcosh}\frac{b}{\xi} \tag{18}$$

and ξ to be the solution of the complementary equation

$$\begin{aligned} c &= c_m(\xi, b) \\ c_m(\xi, b) &= -\frac{2\xi}{L}\sinh\frac{L}{2\xi}\left(\frac{b}{\xi}\sinh\frac{L}{2\xi} - \sqrt{\frac{b^2}{\xi^2} - 1}\cosh\frac{L}{2\xi}\right). \end{aligned} \tag{19}$$

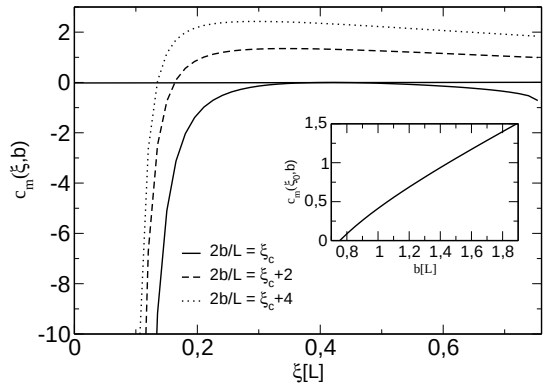

FIG. 1: The upper critical bound for the parameter c according to (19). The inset shows the maximum in dependence on the creeping parameter b.

The solution (17) has not been reported in literature so far and is the main result of this paper.

B. Static stability criteria

Without dynamical bulk charges, $c = 0, d = 1$, the solution (17) is just the well known catenary [20]. The boundary condition (19) reads then

$$\frac{2b}{L} = \frac{2\xi}{L}\cosh\frac{L}{2\xi} \geq \xi_c = 1.5088... \tag{20}$$

which means that without bulk charges the condition for a stable bridge is

$$b > \frac{1}{2}L\xi_c. \tag{21}$$

Together with (2) this condition provides a lower bound for the electric field in order to enable a bridge of length L and has been not discussed so far.

The field-dependent lower bound condition (19) is plotted in figure 1. One see that in order to complete (19) the bulk charge parameter c has to be lower then the maximal value of c_m which reads

$$c \leq c_m(\xi_0, b) \tag{22}$$

and which is plotted in the inset in figure 1. Remembering the definition of the bulk charge parameter (3) we see that (22) sets an upper bound on the bulk charge in dependence on the electric field. The lower bound (21) of the electric field for the case of no bulk charges is obeyed as well since the curve in the inset of figure 1 starts at $b > L\xi_c/2$.

This completes the third question concerning static stability of the bridge. We have found a new catenary solution even for bulk charges in the bridge.

V. DYNAMICAL CONSIDERATION

A. Mass flow of the bridge

We consider now the actual motion of the liquid in the bridge. Here we want to propose the picture that possible charges in the water will move according to the applied electric field and will drag water particles such that a mean mass motion starts. Due to the relatively low Reynolds numbers (40-100) for water we can consider the motion as laminar and we can neglect the convection term $\mathbf{u}\nabla\mathbf{u}$ in the Navier Stokes equation [24] which reads then for the stationary case

$$\eta\nabla^2\mathbf{u} - \rho\nabla p + \rho_c\mathbf{E} = 0. \tag{23}$$

The gradient of the electric pressure (7) can be given in the direction of the bridge by

$$-\nabla p = \frac{\epsilon_0(\epsilon-1)E^2}{2L} = \frac{b}{L}\rho g. \tag{24}$$

Assuming that the flow in the bridge has only a transverse component which is radial dependent, we can solve the Navier Stokes equation like a Poiseullie flow with a resulting velocity profile in the direction of the bridge

$$u(r) = 2u_0\left(\frac{b}{L}+c\right)\left(1-\frac{r^2}{R^2}\right) \tag{25}$$

where R is the radius of the bridge and we have introduced the characteristic velocity (4) using the radius of the water bridge at the beaker (13). The mean current is easily calculated from (25)

$$I = 2\pi\rho\int_0^R drru(r) \equiv \rho v\pi R^2 \tag{26}$$

providing the mean velocity of the bridge as

$$v = u_0\left(\frac{b}{L}+c\right). \tag{27}$$

One sees that the ratio of the field-dependent creeping height (2) to the bridge length determines the mean velocity together with possible dynamical bulk charges described by (3). Please note that the bulk charge transport described by (3) leads to Ohmic behavior and the neutral particle transport due to dielectric pressure leads to a quadratic field dependence condensed in (2). The formula (27) combines the effect of charge transport and neutral particle mass transport. It answers the problem raised in the introduction how the picture of incompressible fluids where the velocity is dependent on the area and Ohmic transport where the velocity is only dependent on the electric field can be thought together.

The resulting total mass current is given in figure 2. The current increases basically with the square of the

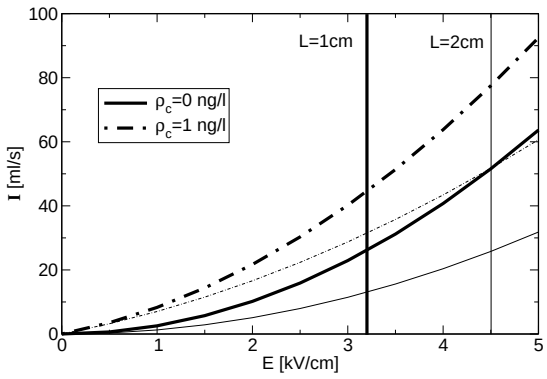

FIG. 2: The mean mass current through the bridge in dependence on the electric field and for two different bulk charge densities. The thick lines are for a bridge length of 1cm and the thin lines for the corresponding length of 2cm. The minimal field strength for stability (21) are indicated by corresponding vertical lines.

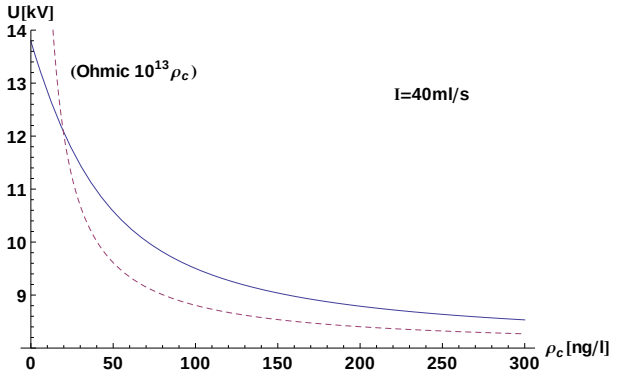

FIG. 3: The necessary applied voltage versus bulk charge densities in order to maintain a mass current of 40ml/s. Following [2] the length of the bridge was $L = 1$cm and the diameter 2.5mm. The result using the flow expression (27) of the present paper (solid line) is compared to an Ohmic transport (broken line). For the latter one the bulk charge has been multiplied with 13 orders of magnitude.

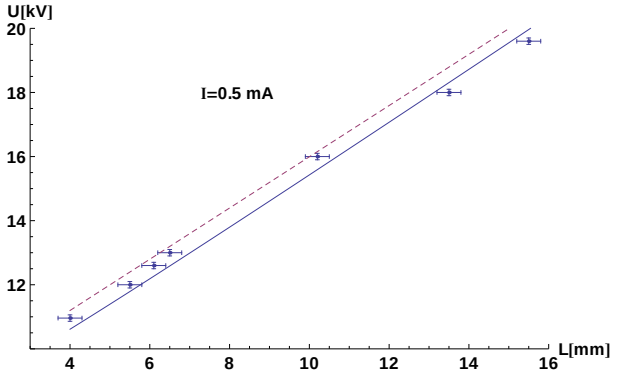

FIG. 4: The necessary applied voltage versus bridge length in order to maintain a charge current of 0.5mA. The data are from figure 6 of [2]. The result using the flow expression (27) and a bulk charge of 2.3ng/l (solid line) is compared to a an Ohmic transport (broken line). For the Ohmic transport the bulk charge has been multiplied with a factor of 3×10^3. The same offset of $U_0 = 8kV$ is used as in the experiments.

applied field scaled by the bridge length. For additional bulk densities the mass flow is higher.

To convince the reader about the validity of the velocity formula (27) we compare now with the mass flow and the charge flow measurements. The experimental values of Figure 4 in [2] are reported to be 40mg/s for a bridge of 1cm length, a diameter of 2.5mm for the stationary regime. For this situation we compare in figure 3 the results obtained from (27) with a pure Ohmic transport using the lowest-order conductivity expression

$$\sigma = \lambda \frac{\rho_c}{eN_A} + \sigma_0 \tag{28}$$

where for clean water the conductivity is σ_0, λ is the molecular conductivity of the solved charge (electrolyte), and N_A the Avogadro constant. We see that our formula (27) leads to a realistic necessary voltage - which was 12.5kV in the experiment - even if no bulk charge is presented. In contrast, for the Ohmic transport one has to assume 13 orders of magnitude higher bulk charges to come into the same range. This illustrates the advantage of the here presented model.

Considering the charge transport we do not expect such big differences of our model to the pure Ohmic picture since the charged particles matters. To this end we compare the applied voltage versus bridge length with a constant charge current as done in figure 6 of [2]. In figure 4 we compare the result from (27) with the pure Ohmic transport. We use a bulk charge of 2.3ng/l. In order to obtain a comparable Ohmic result we had to multiply the bulk charge with a factor of 3×10^3 which illustrates the difference between our model and the Ohmic transport. While the difference in charge transport is not very significant provided the fact that the conductivity of water varies in the order of 3 magnitudes, the mass flow of figure 3 has shown that our result here with (27) is superior since it considers the drag of neutral particles due to dielectric pressure together with the charge transport.

Having the current at hand one estimates the Joule heating easily as

$$\frac{\Delta T}{\Delta t} = \frac{jE}{\rho c_p}. \tag{29}$$

Comparing with the figure 5 of [2] one sees that an increase of 10K in 30min is reported would translate into field strengths of 0.7kV/cm in our calculation. This is much lower than our result. We would obtain here 2-3 orders of magnitude higher heating rates. Please note that the cooling mechanisms like evaporating and cooling due to water flow is beyond the present consideration. Since this is a major cooling effect in experiments [25] we can-

not compare seriously the theoretical heating rate with the experimentally observed ones.

B. Profile of bridge

One can even calculate the profile of the bridge along the length. We consider to this end the total mass flow of the bridge and neglect the viscous term compared to the kinetic energy (which includes part of the convection term), $\mathbf{u}\nabla\mathbf{u} = \frac{1}{2}\nabla u^2 + \mathrm{curl}\mathbf{u}\times\mathbf{u} \approx \frac{1}{2}\nabla u^2$. Then one arrives at the Bernoulli equation

$$\rho\frac{v(x)^2}{2}+\rho g f(x)+\sigma_s(\frac{1}{R(x)})-\rho_c E x = \rho\frac{v^2}{2}+\sigma_s\frac{1}{R}. \quad (30)$$

Here we have neglected the curvature of the bridge compared to the curvature due to the radius and have compared the position-dependent radius $R(x)$ and velocity $v(x)$ in the bridge with the situation at the beaker at $x = 0$. The Bernoulli equation (30) can be rewritten in terms of the capillary height (1) and the velocity (27) as

$$f(x) - cx = \frac{v^2 - v^2(x)}{2g} + a - \frac{a^2}{2R(x)} \quad (31)$$

which determines the radius $R(x)$ from the profile of the bridge (17) and the velocity $v(x)$ if we observe the current conservation through an area

$$R(x)^2 v(x) = R^2 v. \quad (32)$$

The results are presented figure 5. We plot the shape of the bridge, the radius and the velocity together with a 3D plot once for the case of no bulk charges which leads to the standard catenary and once for extreme bulk charges almost at the stability edge (22). We see the deformation of the catenary due to the applied field. This deformation is observed, e.g. if an additional field is brought near the bridge [2, 22]. One sees that the radius is becoming smaller in the middle of the bridge accompanied with higher velocities as it is known from falling water pipes [26]. The bulk charge leads to deformations of this profile which are exaggerated in the plot due to the choice of unequal scales.

Interestingly such asymmetry is experimentally observed [2], where after 3 min of operation the asymmetry for the bridge of 0.9cm length ranges from a diameter of 2.1mm to 2.6mm. This is in agreement with the profile calculated in figure 6. Also the measured asymmetry in the left and right catenary angle [3] in glycerine can be explained with the present model.

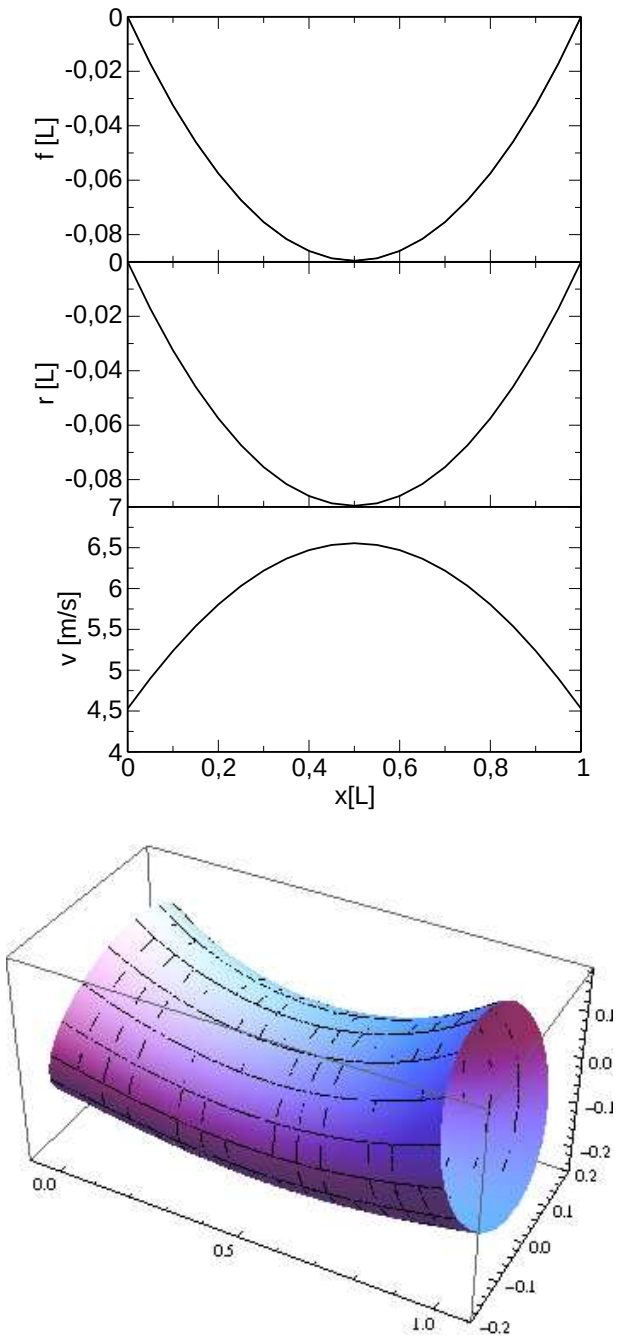

FIG. 5: The center of mass coordinate (above), the radius (middle) and the velocity (bottom) together with the 3D plot of water bridge (in cm) for no bulk charges $c = 0$. The parameter are $b = 1.5$cm and according to table I. Please note the different length scales in x and y, z direction.

C. Dynamical stability

We turn to the question of dynamical stability of the flow and consider the motion of water together with the motion of charged particles characterized by the mass m_i and charge e_i. This charge current is given by Ohm's law σE and the corresponding mass current can be written

$$j_i = \frac{m_i}{e_i} j = x_i \frac{\rho}{\rho_c}\sigma E \quad (33)$$

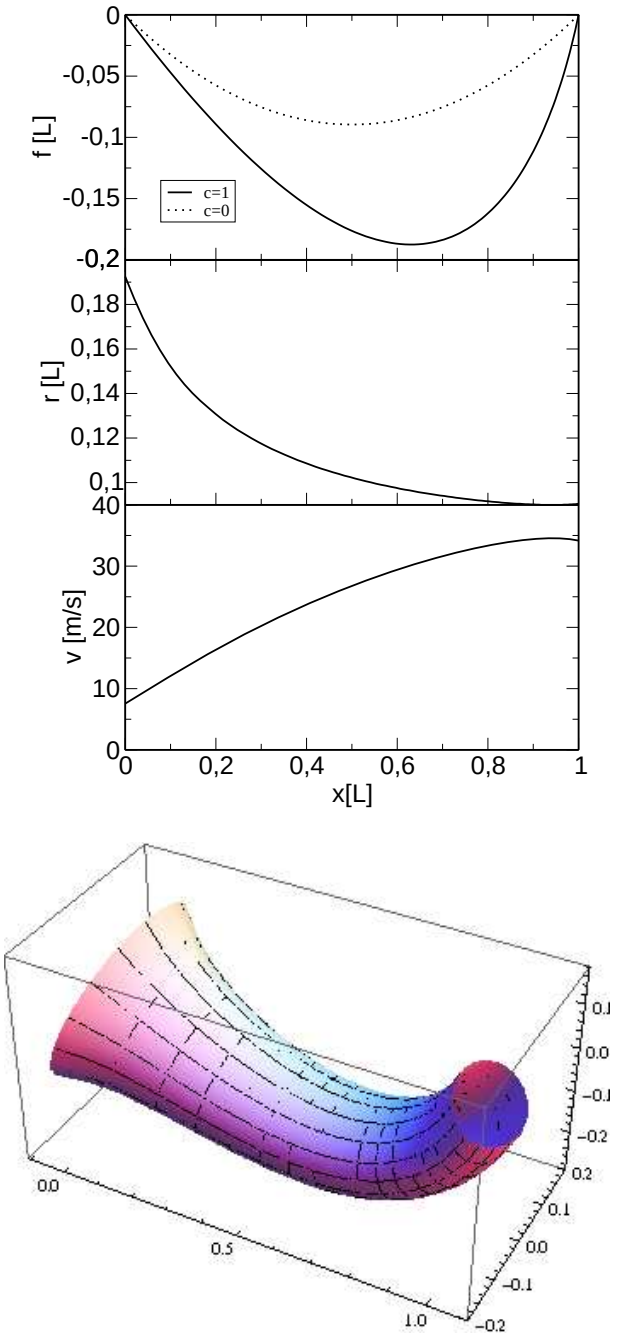

FIG. 6: The center of mass coordinate (above), the radius (middle) and the velocity (bottom) together with the 3D plot of water bridge (in cm) with bulk charges $c = 1$. The parameter are $b = 1$cm and according to table I.

where we introduced the mass ratio of the number of charged particles (e.g. NaCl) to the water particles

$$x_i = \frac{\#_i m_{\rm NaCl}}{\#_w m_{\rm H_20}} = \frac{\rho_c m_i}{\rho e_i}. \tag{34}$$

The mass current of the neutral (water) particles are

$$j_n = \rho_n v_n = (\rho - \frac{m_i}{e_i}\rho_c)v_n = (1 - x_i)\rho v_n \tag{35}$$

such that the total mass current reads

$$\rho v = j_i + j_n = x_i \frac{\rho}{\rho_c}\sigma E + (1 - x_i)\rho v_n. \tag{36}$$

The total current (left side) should be larger than the current only from the charged particle (last term right side). However the velocity of charged particles, $\sigma E/\rho_c$ should be larger than the velocity of the dragged water molecules v_n and therefore larger than the mean velocity v of the mass motion. Together with (27) this is expressed by the inequality

$$\frac{\sigma E}{\rho_c} > u_0 \left(\frac{b}{L} + c\right) > x_i \frac{\sigma E}{\rho_c} \tag{37}$$

which gives an upper and lower bound on the possible mass motion created by the drag of particles due to the force on charged particles.

If we now take into account the dependence of the conductivity on the density of the solved ions in water we can find a condition on possible bulk charges in water to maintain a stable bridge. To this aim we consider very small charge densities solved in water which allows to consider the lowest order dependence of the conductivity on the bulk charge concentration (28).

Noting the charge-density dependencies of x_i, b and c via (34), (2) and (3) one obtains from (37) the dynamical restriction on possible bulk charges

$$\begin{aligned} \rho_c \ &\in \ \rho_1 - \rho_2 \pm \sqrt{(\rho_1 - \rho_2)^2 + \rho_3^2} \\ \rho_c(1 - 2\rho_2/\rho_i) \ &> \ \rho_3^2/\rho_i - 2\rho_1 \end{aligned} \tag{38}$$

with the auxiliary densities

$$\begin{aligned} \rho_1 \ &= \ \epsilon_0(\epsilon - 1)\frac{E}{2L}, \quad \rho_2 = \frac{16\eta\lambda}{eN_A a^2} \\ \rho_3^2 \ &= \ \frac{32\eta\sigma_0}{a^2}, \quad \rho_i = \frac{e_i\rho}{m_i}. \end{aligned} \tag{39}$$

The results for NaCl in water (table I) are plotted in figures 7-8. The static stability condition (21) gives the upper and charge-density-independent limit in figure 8. The static condition (22) with bulk charges leads to the border of maximal densities on the right side which agrees with (21) at zero densities, of course. The lower minimal length of the bridge at a given field strength and bulk charge is provided by the dynamical condition (38). For no bulk charge the possible range of lengths of the bridge starts at zero and is limited by the upper length (21). If there are charges present, there is a minimal length required to have a stable bridge.

From the 3D plot in figure 8 one can see that for finite charges and fixed bridge length there is a lower and an upper critical field where bridges can be stable. From the experiments [2] it is seen that the bridge forms jets for fields higher than 15kV/cm.

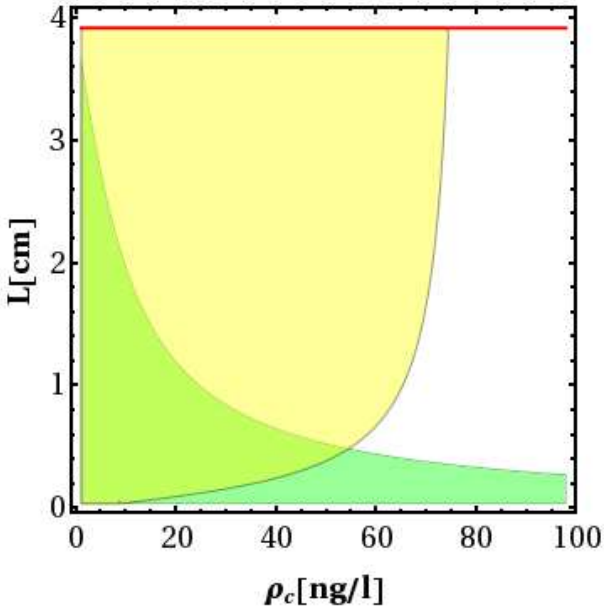

FIG. 7: The range of possible water bridges for an electric field of $E = 0.64$kVcm. Upper limit due to static stability condition (22) and lower cut due to dynamical condition (38). The bulk charge free condition is the upper straight line.

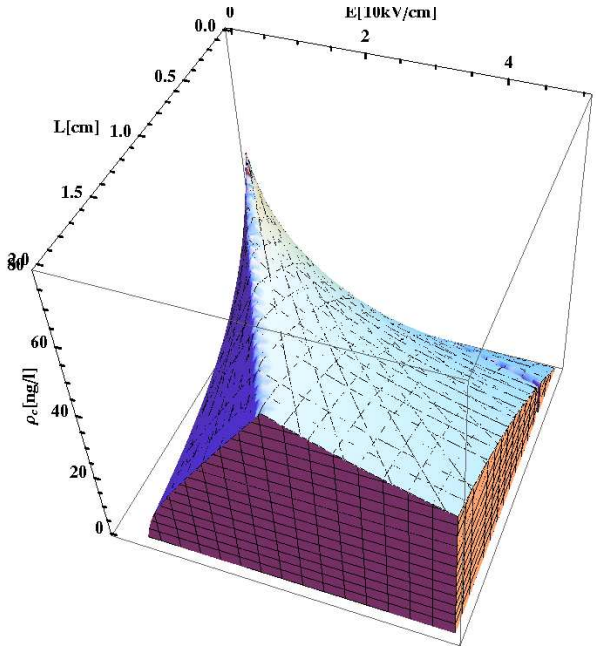

FIG. 8: The range of possible water bridges in dependence on bridge length, electric field and electrolyte bulk charges.

VI. SUMMARY

The formation of water bridges between two vessels when an electric field is applied has been investigated macroscopically. Electrohydrodynamics is sufficient to describe the phenomena in agreement with the experimental data. The four necessary parameters which are build up from microscopic properties of the charged liquid are the capillary height (1), the creeping height (2), the dimensionless ratio between field and gravitational force density (3), and the characteristic velocity (4).

As new contribution to the discussion, an exact solution has been found of the charged catenary which was not reported so far. This leads to a static stability criterion for possible charges in the liquid dependent on the applied field strengths and length of the bridge. With no bulk charge present the maximal bridge length is determined and no minimal length occurs. This changes if bulk charges are present. Then also a minimal length is required. However, only very small concentrations of bulk charges are possible and the bridge is easily destroyed when bulk charges in the order of 50 ng/l are present. As a further result it is obtained an asymmetric profile in the diameter along the bridge which was observed by asymmetric heating.

For the dynamical consideration a picture is proposed of dragged liquid particles due to the motion of the charged ones besides the ponderomotoric forces due to the dielectric character of the liquid. The resulting dynamical stability consideration restricts the possible parameter range of bridge formation. The resulting mass flow combines the charge transport and the neutral mass flow dragged by dielectric pressure and is in agreement with the experimental data.

The presented simple classical theory applies for charged liquids as long as the Reynolds number is such low that laminar flow can be assumed.

Acknowledgments

The discussions with Burn Kutschan who pointed out this interesting effect to me and the clarifying comments of Jacob Woisetschläger are gratefully mentioned. This work was supported by DFG-CNPq project 444BRA-113/57/0-1 and the DAAD-PPP (BMBF) program. The financial support by the Brazilian Ministry of Science and Technology is acknowledged.

[1] W. G. Armstrong, *The Electrical Engineer* (The Newcastle Literary and Philosophical Society, New Castle, 1893), pp. 154–155, 18 February 1893.

[2] J. Woisetschlager, K. Gatterer, and E. Fuchs, Exp. in Fluids **48**, 121 (2010).

[3] A. G. Marin and D. Lose, Phys. of Fluids **22**, 122104 (2010).

[4] G. Sacha, A. Verdaguer, and M. Salmeron, J. Phys. Chem. B **110**, 14870 (2006).

[5] J. M. Oh, S. H. Ko, and K. H. Kang, Physics of Fluids

p. 032002 (2010).
[6] A. Garcia-Martin and R. Garcia, Appl. Phys. Lett. **88**, 123115 (2006).
[7] S. Gomez-Monivas, J. Saenz, M. Calleja, and R. Garcia, Phys. Rev. Lett. **91** (2003).
[8] T. Cramer, F. Zerbetto, and R. Garcia, Langmuir **24**, 6116 (2008).
[9] S. Chen, X. Huang, N. F. A. van der Vegt, W. Wen, and P. Sheng, Phys. Rev. Lett. **105**, 046001 (2010).
[10] T. Squires and S. Quake, Rev. Mod. Phys. **77**, 977 (2005).
[11] A. Ganancalvo, J. of Fluid Mechanics **335**, 165 (1997).
[12] M. Gamero-Castano, J. of Fluid Mechanics **662**, 493 (2010).
[13] F. Higuera, Physics of Fluids p. 112107 (9 pp.) (2010).
[14] J. Eggers, Phys. Rev. Lett. **71**, 3458 (1993).
[15] J. Eggers, Rev. Mod. Phys. **69**, 865 (1997).
[16] F. Saija, F. Aliotta, M. Fontanella, M. Pochylski, G. Salvato, C. Vasi, and R. Ponterio, J. of Chem. Phys. **133**, 081104 (2010).
[17] J. Melcher and G. Taylor, Ann. Rev. of Fluid Mech. **1**, 111 (1969).
[18] L. D. Landau and E. M. Lifschitz, *Lehrbuch der Theoretischen Physik: Elektrodynamik der Kontinua*, vol. VIII (Akademie-Verlag, Berlin, 1990).
[19] A. Ramos, H. Morgan, N. Green, and A. Castellanos, J. Phys. D - Appl. Phys. **31**, 2338 (1998).
[20] A. Widom, J. Swain, J. Silverberg, S. Sivasubramanian, and Y. Srivastava, Phys. Rev. E **80** (2009).
[21] L. Giuliani, E. D'emilia, A. Lisi, S. Grimaldi, A. Foletti, and E. Del giudice, Neural Network World **19**, 393 (2009).
[22] E. Fuchs, J. Woisetschlager, K. Gatterer, E. Maier, R. Pecnik, G. Holler, and H. Eisenkolbl, J. Phys. D - Appl. Phys. **40**, 6112 (2007).
[23] D. E. Moulton and J. A. Pelesko, Siam J. on Appl. Math. **70**, 212 (2009).
[24] D. S. Chandrasekharaiah, *Contuum mechanics* (Academic Press, Boston, 1994).
[25] J. Woisetschlager, priv. communication.
[26] M. J. Hancock and J. W. Bush, J. Fluid Mech. **466**, 285 (2002).